

UCLA

UCLA Previously Published Works

Title

Exceptional aggressiveness of cerebral cavernous malformation disease associated with PDCD10 mutations.

Permalink

<https://escholarship.org/uc/item/0cs6m4h5>

Journal

Genetics in medicine : official journal of the American College of Medical Genetics, 17(3)

ISSN

1098-3600

Authors

Shenkar, Robert
Shi, Changbin
Rebeiz, Tania
et al.

Publication Date

2015-03-01

DOI

10.1038/gim.2014.97

Peer reviewed



Published in final edited form as:

Genet Med. 2015 March ; 17(3): 188–196. doi:10.1038/gim.2014.97.

EXCEPTIONAL AGGRESSIVENESS OF CEREBRAL CAVERNOUS MALFORMATION DISEASE ASSOCIATED WITH *PDCD10* MUTATIONS

Robert Shenkar, PhD^{#1}, Changbin Shi, MD, PhD^{#1}, Tania Rebeiz, MD², Rebecca A. Stockton, PhD³, David A. McDonald, PhD^{4,5}, Abdul Ghani Mikati, MD¹, Lingjiao Zhang, MS¹, Cecilia Austin, BS¹, Amy L. Akers, PhD⁶, Carol J. Gallione, BA⁴, Autumn Rorrer, BA⁴, Murat Gunel, MD⁷, Wang Min, PhD⁸, Jorge Marcondes De Souza, MD, PhD⁹, Connie Lee, PsyD⁶, Douglas A. Marchuk, PhD^{#4}, and Issam A. Awad, MD, MSc^{#1,2}

¹Neurovascular Surgery Program, Section of Neurosurgery, The University of Chicago Medicine, Chicago, IL 60637, USA

²Department of Neurology, The University of Chicago Medicine, Chicago, IL 60637, USA

³Department of Pediatrics, University of California at Los Angeles, Torrance, CA 90502, USA

⁴Department of Molecular Genetics and Microbiology, Duke University, Durham, NC 27710, USA

⁵Center for Science, Math and Technology Education, North Carolina Central University, Durham, NC 27707, USA

⁶Angioma Alliance, Norfolk, VA 23510, USA

⁷Departments of Neurosurgery and Neurobiology, Yale University, New Haven, CT 06520, USA

⁸Department of Pathology, Yale University, New Haven, CT 06520, USA

⁹Department of Neurosurgery, School of Medicine, Federal University of Rio De Janeiro, Rio de Janeiro, Brazil

[#] These authors contributed equally to this work.

Abstract

Purpose—The phenotypic manifestations of cerebral cavernous malformation (CCM) disease caused by rare *PDCD10* mutations have not been systematically examined, and a mechanistic link to Rho kinase (ROCK) mediated hyperpermeability, a potential therapeutic target, has not been established.

Users may view, print, copy, and download text and data-mine the content in such documents, for the purposes of academic research, subject always to the full Conditions of use: http://www.nature.com/authors/editorial_policies/license.html#terms

Correspondence should be addressed to: Section of Neurosurgery, The University of Chicago, 5841 S. Maryland, MC 3026, Chicago, IL 60637 USA. Tel: +1 7737022123; Fax: +1 7737023518; iawad@uchicago.edu.

DISCLOSURE

The authors have declared that no conflict of interest exists.

SUPPLEMENTARY MATERIAL

Supplementary material is linked to the online version of the paper at the *Genetics in Medicine* website <http://www.nature.com/gim>

Methods—We analyze *PDCD10*-siRNA treated endothelial cells for stress fibers, ROCK activity and permeability. ROCK activity is assessed in CCM lesions. Brain permeability and CCM lesion burden is quantified, and clinical manifestations are assessed in prospectively enrolled subjects with *PDCD10* mutations.

Results—We determine that *PDCD10* protein suppresses endothelial stress fibers, ROCK activity and permeability *in vitro*. *Pdcd10* heterozygous mice have greater lesion burden than other *Ccm* genotypes. We demonstrate robust ROCK activity in murine and human CCM vasculature, and increased brain vascular permeability in humans with *PDCD10* mutation. Clinical phenotype is exceptionally aggressive compared to the more common *KRIT1* and *CCM2* familial and sporadic CCM, with greater lesion burden and more frequent hemorrhages earlier in life. We first report other phenotypic features including scoliosis, cognitive disability and skin lesions, unrelated to lesion burden or bleeding.

Conclusion—These findings define a unique CCM disease with exceptional aggressiveness, and they inform preclinical therapeutic testing, clinical counseling and the design of trials.

Keywords

Cerebral cavernous malformations; vascular malformations; *PDCD10*; *CCM3*; Rho kinase

INTRODUCTION

Cerebral cavernous malformations (CCM) are clusters of grossly dilated brittle capillaries, predisposing patients to a lifetime risk of hemorrhagic stroke, epilepsy and other sequelae¹. Familial forms account for about a third of cases, involving autosomal dominant inheritance at one of three gene loci². No current treatment exists for CCM, except highly invasive surgical procedures for resecting symptomatic lesions. Despite promising pharmacotherapeutic targets³⁻⁵, progress to clinical trials has been hindered by the relatively benign manifestations of CCM disease in general, a low rate of new lesion development, and the unpredictability of serious clinical events⁶⁻⁸.

Few studies have examined any special features of the rarest cases with programmed cell death 10 (*PDCD10*) mutation (also known as the *CCM3* locus), constituting <15 % of probands genotyped by sequential mutation screening, and <2% of CCM cases at large. Our group and others have suggested different disease aggressiveness with various CCM genotypes⁹⁻¹¹, and bleeding at young age and meningiomas were recently associated with *PDCD10* cases¹². But there has been no systematic assessment of lesion burden, hemorrhage risks per lesion and per patient, nor other comprehensive phenotypic survey in probands with this mutation. The potential link of Rho kinase (ROCK) activity to the loss of *PDCD10* protein had been suggested previously^{13, 14}, but it has not been linked to vascular hyperpermeability as with other CCM genotypes¹⁵. ROCK activity has not been previously examined in vascular lesions from these patients, nor their brain permeability *in vivo*. And other reports have suggested that *PDCD10* mutations might cause CCM via distinct Rho independent mechanisms¹⁶⁻²⁰.

Herein we confirm that *PDCD10* loss is associated with increased ROCK activity, stress fiber induction and endothelial permeability *in vitro*, rescued by ROCK inhibition. And we demonstrate ROCK activity in CCM vasculature in mouse and humans, defining a mechanistic link and a potential therapeutic target. We show that *Pdcd10/PDCD10* mutations result in significantly greater lesion burden in mouse and humans than other CCM disease, more severe clinical manifestations, and document several novel clinical associations. We first report that the brain of *PDCD10* patients manifests vascular hyperpermeability, confirming the expected impact of ROCK activity *in vivo*. The exceptionally high rates of lesion formation and symptomatic hemorrhage motivate novel hypotheses for mechanistic studies, and provide an opportunity to focus preclinical optimization and early therapeutic trials on this small but seriously affected subgroup of CCM cases.

MATERIALS AND METHODS

Details for human subjects, cell culture, the *Pdcd10*^{+/-}*Trp53*^{-/-} heterozygous murine model, genetic testing in subjects, transfection, immunofluorescence, western blotting, RhoA activation assay, permeability assay *in vitro*, sample preparation and histology, immunohistochemistry, lesion burden and *in vivo* brain permeability in humans, lesion burden and clinical features, and statistical methods and control comparisons are provided in Supplementary Materials and Methods online. Methods have been described previously for assessment of endothelial barrier function *in vitro*¹⁵, preparation of murine brain sections³ and ROCK activity assays^{3, 15}.

RESULTS

PDCD10 inhibits ROCK and maintains endothelial barrier function

Knockdown efficacy was approximately 80% reduction in *PDCD10* message in human umbilical vein endothelial cells (HUVECs) transfected with *PDCD10* siRNA (Figure 1A). Control and *PDCD10* si-RNA-treated HUVECs were stained for f-actin to show the extent of stress fiber content (Figure 1B). Stress fiber content was increased with PDCD10 depletion. This increase was reversed by the ROCK inhibitor, H-1152. These effects were confirmed in human brain microvascular cells (hbmVEC), when *KRIT1*, *CCM2* or *PDCD10* si-RNA was used (Supplementary Figure S1 online). A consequence of ROCK activation is phosphorylation of myosin light chain (MLC). To monitor ROCK activity, control and *PDCD10* si-RNA-treated HUVECs were stained for phosphorylated MLC (pMLC) after Western blotting (Figure 1C). PDCD10 depletion increased ROCK activity, which was suppressed by H-1152. These effects were confirmed in hbmVEC, while total MLC levels were not affected by PDCD10 depletion or H-1152 (Supplementary Figure S2 online). Rho-GTP activity was increased after *KRIT1*, *CCM2* or *PDCD10* knockdown (Supplementary Figure S3 online). Stability of endothelial cell junctions was measured by permeability of control and *PDCD10* si-RNA-treated HUVEC monolayers (Figure 1D). Upon PDCD10 depletion the monolayers became more permeable. This increased leakage was reversed by H-1152, indicating rescue of the hyperpermeable endothelial phenotype by ROCK inhibition, despite PDCD10 loss.

Pdcd10 heterozygous mouse models have more numerous and larger CCM lesions

Total lesion burden per mouse was significantly greater ($P<0.001$) when comparing 15 *Pdcd10*^{+/-} sensitized animals in the *Trp53*^{-/-} background, to 53 mice with other heterozygous CCM genotypes (*Krit1*^{+/-} or *Ccm2*^{+/-}) in the same backgrounds (Supplementary Table S1 online). The sensitized *Pdcd10*^{+/-}*Trp53*^{-/-} model had over sevenfold more prevalent CCM lesions, than similarly sensitized models of *Krit1*^{+/-}*Trp53*^{-/-} or *Ccm2*^{+/-}*Trp53*^{-/-} genotypes, and also a greater burden of mature stage 2 lesions.

Even non-sensitized *Pdcd10*^{+/-} mice (without *Trp53* loss) manifested typical CCM lesions (mean 1.6 lesions/mouse), while no such lesions were documented in non-sensitized heterozygotes of other CCM genotypes ($P<0.001$). The mean area for the stage 2 lesions was larger in the *Pdcd10*^{+/-}*Trp53*^{-/-} model (0.94 mm² per lesion) than in other sensitized genotypes (0.34 mm²/lesion) ($P<0.01$). From these mouse models, it is clear that heterozygous loss of *Pdcd10*, with or without genetic sensitization, leads to a more severe and penetrant CCM phenotype than loss of either *Krit1* or *Ccm2*.

Cerebral endothelial cell ROCK activity is present in Pdcd10 heterozygous mice

ROCK activity was present in CCM lesions and in background capillaries in both sensitized and non-sensitized *Pdcd10* models as assessed by staining of pMLC and phosphorylated myosin binding substrate (pMBS) (Supplementary Figure S4 online), whereas no such activity is seen in capillaries of wild type control mice²¹. The prevalence of pMLC immunopositive caverns was the same in CCM lesions regardless of sensitized or non-sensitized background (95.4% of 1111 caverns counted in 79 lesions present in five *Pdcd10*^{+/-}*Trp53*^{-/-} mice versus 96.5% of 142 caverns counted in 23 lesions in eleven non-sensitized *Pdcd10*^{+/-} mice), indicating that ROCK activity in CCM lesions is related to the *Pdcd10* mutations and not the background sensitizer. These results complement our *in vitro* experiments by demonstrating the impact of *Pdcd10* mutations on ROCK activity *in vivo*.

Cerebral endothelial ROCK activity in human CCM lesions

We demonstrated ROCK activity in human *PDCD10* CCM lesions, as in murine lesions. Human *PDCD10* CCM lesions had twice as many caverns with ROCK activity than human *KRIT1*, *CCM2* and sporadic CCM lesions ($P<0.05$) (Figure 2).

Spectrum of mutations in PDCD10 in humans, prevalence of spontaneous mutations

The allelic series of *PDCD10* mutations is catalogued in Table 1. All mutations are predicted to lead to a loss of function allele. In 12 of 13 probands, mutations included nonsense and splice site altering mutations. Proband number 12 carried a missense mutation, c.131T>C; p.Leu44Pro. This helix-breaking mutation is predicted to result in loss of function by disrupting helix α C of the PDCD10 protein, thereby inhibiting both PDCD10 homo-dimerization and binding to the GCKIII kinases²². Sixteen of the 18 patients underwent parental screening for their index *PDCD10* mutation. Seven of the 16 cases with parental screening (44%) harbored a spontaneous, *de novo* mutation not inherited from either parent.

Early onset hemorrhage and high risk of recurrent bleeds in humans

The mean age of first clinical symptom was 12.6 years (range 0.25-52). Symptomatic CCM bleed was the most common presenting event, affecting ten of 18 subjects (56%), who suffered 37 overt hemorrhages. Estimated incidence of hemorrhage was 7.9% (CI 5.6 - 11) per patient per year based on exposure risk since birth, and 20% (CI 14 - 28) per patient per year based on risk since first symptom onset. The risk of recurrent bleed after a first bleed was 24% per patient per year (CI 16 - 35). There were significant associations between the annual bleed rate and a younger age at first symptom onset, age at first bleed and a younger age at diagnosis ($P<0.001$, respectively), but no significant difference between sexes. Life tables of hemorrhage risk from birth, from first symptom, and from first bleed are presented in Figure 3A and 3B.

The first overt hemorrhage occurred most often in the first decade of life (mean age 5.9, range 0.33-12). This is significantly earlier than the age at first bleed in *KRIT1* and *CCM2* familial cases evaluated in our clinic (mean age 30, range 1-52, $P<0.05$), and in the clinical dataset for the Angioma Alliance DNA/Tissue Bank (mean age 32, range 3-55, $P<0.001$) (Figure 3C and Supplementary Figure S5 online).

Exceptional lesion burden in humans as in mouse, with low bleeding rate per lesion

Lesion burden on susceptibility weighted imaging (SWI) was exceptionally high, with 33% of *PDCD10* cases harboring >100 lesions and 78% harboring > 20 lesions. The mean number of lesions per patient on T2-weighted magnetic resonance imaging (MRI) scan was 31.33 (CI 20.64 to 47.57) in *PDCD10* cases, significantly greater than the mean lesion count of 5.25 (CI 2.38 to 11.59) in familial *KRIT1* and *CCM2* cases ($P<0.001$). When adjusted for age, the SWI lesion burden was also significantly greater in the *PDCD10* cohort than in control familial cases with *KRIT1* or *CCM2* mutations (2.03 SWI lesions/year of life in *PDCD10* versus 1.08 in *KRIT1* and *CCM2* cases, $P<0.01$). *PDCD10* patients form 2.36 new lesions on T2 per year of follow up compared to 0.30 new lesions per year of follow up in *KRIT1* cases ($P=0.002$). Among nine cases that underwent 19 prospective repeated MRI scans with comparable technique, there were 2.7 (CI 1.8-3.9) new SWI lesions per patient per year of follow up. An MRI scan from one such case with exceptionally high SWI lesion burden is shown in Figure 3D.

Bleeding rate per lesion per year after first symptom onset was 0.3 % (CI 0.2-0.4), similar to that previously reported in other CCM genotypes^{6-8, 23-25}. The rebleeding rate per lesion after a first bleed from any lesion was only slightly higher at 0.4 % (CI 0.23-0.52). This suggests that the high bleeding rate in *PDCD10* subjects is due to the exceptional lesion burden, rather than any particularly higher hemorrhagic propensity of individual CCM lesions. CCM lesions in SWI scans formed at a rate of 2.03 lesions (CI 1.89 - 2.16) per patient per year of life.

Increased brain permeability in humans

Using dynamic contrast enhanced quantitative perfusion (Supplementary Figure S6 online), patients with *PDCD10* mutations exhibited increased permeability in white matter far from the lesions compared to sporadic CCM cases without germline mutations ($P<0.05$). This

finding was also observed in other familial cases (unpublished data). Lesional permeability in *PDCD10* cases was found to be higher than in *KRIT1* cases. This confirms a functional impact of ROCK activity associated with *PDCD10* mutations *in vivo*.

Other clinical features of PDCD10 mutation

Figure 4 illustrates each symptomatic bleed noted during the lifespan of each subject, groups the cases by their respective proband, and presents relevant information about each subject's lesion burden and clinical associations.

Skin lesions were noted in five cases (28%). Two patients had café-au-lait lesions, one had a scalp hemangioma, and two patients had cutaneous cavernous malformations (both confirmed by biopsy). Scoliosis was documented in seven cases (39%). Three of these patients had spinal fusion due to severe scoliosis. Of those seven cases, two underwent spinal MRI scans, and one was noted to harbor a spinal cord CCM lesion. The presence of scoliosis was significantly associated with the rate of recurrent bleed per year after a first documented hemorrhage ($P=0.001$), and with the rate of bleed per lesion per year after a first bleed ($P=0.001$). There was no association between the presence of skin lesions or scoliosis and lesion burden, cumulative bleeds per case, the annual bleeding rate, the age at onset of first symptoms, nor the age at first bleed.

A brain tumor was found in five cases (28%). Based on MRI features, this had the dural-based appearance of meningioma in two subjects, and the intra-canalicular nodular appearance of acoustic neuroma in two subjects. An additional subject had a biopsy-proven cerebellar astrocytoma. The presence of brain tumor was significantly associated with the rate of recurrent bleed per year after a first documented hemorrhage ($P<0.001$), and with the rate of bleed per lesion per year after a first bleed ($P<0.001$). However, there was no association of tumor with lesion burden, cumulative bleeds per case, the annual bleeding rate, the age at onset of first symptoms, nor the age at first bleed. After Bonferroni correction, scoliosis and brain tumor association with bleeds per year after a first bleed, and with bleeds per lesion per year after the first bleed were all significant at $P<0.01$.

Cognitive disability was present in 11 cases (61%) including a learning disorder most commonly noted in eight pediatric cases. Surprisingly, we documented no association between the presence of cognitive disability and lesion burden, cumulative bleeds per case, the annual bleeding rate, the age at onset of first symptoms, nor the age at first bleed. Lesion burden may not necessarily result from increased loss of heterozygosity (LOH) for the *PDCD10* gene. *PDCD10* protein may act through a different mechanism than *KRIT1/CCM2* proteins¹⁶⁻²⁰.

DISCUSSION

Two critical questions were answered in this study, establishing that *PDCD10* mutations result in vascular permeability mediated by ROCK activity, and a particularly severe clinical phenotype with previously unappreciated features. Other mechanistic questions remain unanswered, with current results generating a number of novel hypotheses.

It was shown in recent years that mutations in CCM genes *KRIT1* and *CCM2* result in stress fiber expression and endothelial barrier leak, mediated by ROCK activation^{15, 26}. In fact, ROCK³ or broader Rho⁵ inhibition have been advocated as potential therapeutic strategies. Although there is no *in vivo* confirmation that RhoA is associated with disease manifestations, our data suggest ROCK may be involved in *PDCD10* disease. But it has been suggested that *PDCD10* mutations may cause CCM disease via a different mechanism¹⁶⁻²⁰. Vascular permeability and ROCK activity had not been systematically explored as a result of *PDCD10* loss. Brain permeability by MRI with ROCK activity is presently being investigated in our laboratory in humans with familial CCM. We now confirm the expression of stress fibers, endothelial hyperpermeability, and increased ROCK activity with loss of *PDCD10*, as we had shown previously with the more common *KRIT1* gene^{3, 15}. We also demonstrate phenotype rescue *in vitro* with ROCK inhibition, despite *PDCD10* loss, consistent with a report by Borikova *et al.*¹⁴.

We add other pieces of critical information, including the demonstration of increased ROCK activity in normal background vessels and in CCM lesions in man and mouse in sensitized background. Mice heterozygous for CCM genes have been shown to manifest hyperpermeability in several vascular beds, including the brain of murine models^{15, 26}. For the first time, we document increased brain permeability in the white matter of humans with heterozygous *PDCD10* mutations.

Interesting information was gleaned by comparing lesion burden in *Pdcd10* heterozygous mice and our previously reported heterozygous *Krit1* or *Ccm2* murine models recapitulating the human disease. We had previously shown no detectable CCM lesions in *Krit1* or *Ccm2* heterozygous mice, except when sensitized with the loss of tumor suppression (*Trp53*) or DNA point mutation repair (*Msh2*) genes^{21, 29}, consistent with enhanced lesion genesis as a result of Knudsonian second-hit somatic mutations^{30, 31}. In contrast, *Pdcd10* heterozygous mice manifest typical CCM lesions without such sensitization, suggesting a much more penetrant phenotype. Indeed, comparably sensitized heterozygous *Pdcd10* models manifest a tenfold greater lesion burden than other CCM genotypes.

Other studies had indicated bleeding earlier in life with this genotype^{9, 11, 12}. We now provide a systematic correlation with lesion burden, the rate of lesion formation, and hemorrhagic risk. These discoveries would not have been possible, without the concerted efforts of Angioma Alliance at facilitated referral of every known case of *PDCD10* mutation in the United States, to a single specialized clinic performing systematic genotyping, phenotypic screening, advanced imaging and biomarker studies. This represents a model of studying rare diseases, although we acknowledge potential bias despite best currently available controls. As with mice, we show that patients affected with *PDCD10* mutations have an exceptionally greater lesion burden, and more frequent bleeding episodes than other CCM genotypes. They form new small SWI lesions at about twice the rate per year of life, and more clinically relevant T2 lesions on MRI at more than six-fold. Remarkably, each CCM lesion is associated with a very low risk of hemorrhage per year, in the 0.3% range, as was reported with other genotypes^{6, 7, 23-25}. Hence the bleeding tendency in the *PDCD10* genotype appears to result from a much greater number of lesions, rather than any special lesional vulnerability to hemorrhage. This favors therapeutic targeting of lesion burden, or

the prevention of lesion development early in life. Patients who have had a first documented symptomatic CCM hemorrhage are often in the first decade of life, and are predisposed to recurrent bleeds at a rate greater than 20% per year, higher than any reported with other CCM genotypes.

We document a high frequency of spontaneous mutation in this disease, reflecting in part the very severe phenotype (disability at young age preventing procreation), and consistent with the previously reported less numerous affected relatives as compared to other familial CCM cases^{2, 11, 32}. Two mutations, c.474+5G>A and c.474+1G>A were present respectively in three and two unrelated families. A potential founder effect with these mutations will need to be examined.

The high rates of CCM lesion formation, assuming each lesion represents a separate somatic mutation event, implies that the *PDCD10* locus may be prone to deleterious mutations, possibly representing a mutation hotspot. Many of the second-hit somatic mutations are likely due to LOH generated by mitotic recombination. The location of the three CCM genes on their respective chromosomes in both human and mouse supports a higher frequency of mitotic recombination for the *CCM3/Ccm3* genes. For the human, the *KRIT1/CCM2* gene is located on the q arm approximately 32 Mb from the centromere of chromosome 7, the *CCM2* gene is located approximately 15 Mb from the same centromere on the p arm of chromosome 7, whereas the *PDCD10/CCM3* gene is located on the q arm approximately 76 Mb from the centromere of chromosome 3 (GRCh38 assembly). In the mouse, the *Krit1/Ccm1* gene is located approximately 3.8 Mb from the telocentric centromere on chromosome 5, the *Ccm2* gene is located approximately 6.6 Mb from the telocentric centromere on chromosome 11, whereas the *Pdcd10/Ccm3* gene is located approximately 75 Mb from the telocentric centromere on chromosome 3 (GRCm38 assembly). The larger distance from their respective centromeres to the *CCM3/Ccm3* gene in both species provides the genetic template for an increased opportunity for mitotic recombination, leading to LOH and the initiation of CCM lesion development. Further study of the molecular genetic cause of this phenomenon is needed, potentially explaining the exceptional disease aggressiveness. There was substantial variability in lesion burden, bleeding and associated phenotypic features among subjects, among families and even within respective probands. Factors impacting disease aggressiveness, including potential genetic and epigenetic modifiers merit further investigation.

It may be questioned whether the each CCM lesion in these patients is the result of a separate and unique somatic mutation. The number of cell divisions and spontaneous mutations necessary during each replication cycle to generate the abundance of lesions many not be possible during the short timeframe of lesion genesis in many of these patients' lifespan. While somatic biallelic loss of *PDCD10* has been shown in human lesions from familial cases with germline *PDCD10* heterozygosity³¹, this may not be a requirement for the genesis of every lesion, particularly in the setting of this highly prolific genotype. This will require further investigation, including the sequencing of multiple lesion samples from the same patient or mouse. It is also possible that *PDCD10* may act as a tumor suppressor, inherently sensitizing patients to somatic mutations, and this could also explain the

association of tumors with this CCM genotype (see below). This mechanism will require further investigation.

Other phenotypic features are intriguing. An association with skin lesions had been reported primarily with *KRIT1* cases³³. We now report it with *PDCD10* cases, although the lesions are different (more café-au-lait lesions, for example, rather than keratotic angiomas). Associated meningiomas have also been reported¹², but we herein document other brain tumors as well. Finally, scoliosis and cognitive impairment are first reported here, in association with this unique cohort. Scoliosis may or may not be due to associated spinal lesions, it was not associated with myelopathy, as would be expected with spinal CCMs, and one of two cases with severe scoliosis who underwent spinal MRI had no evidence of spinal CCM lesions. The frequency of disabling cognitive impairment is equally sobering. These novel phenotypic features require further investigation, yet we note no specific relationship of scoliosis or cognitive disability with lesion burden or hemorrhage. This motivates hypotheses about the impact of *PDCD10* loss on skeletal integrity and neurocognitive development or function. These effects might be related to other postulated fundamental roles of *PDCD10* in cell orientation and Golgi assembly¹⁷, DLL4-Notch signaling¹⁸, and more recently neuronal migration¹³. We herein note that cognitive impairment in senescence has also been correlated with vascular permeability and ROCK activity³⁴.

In contrast to most CCM patients with other genotypes, who often live normal lives with infrequent and rarely disabling clinical events, patients with *PDCD10* mutations are frequently devastated by lesion burden and repeated hemorrhages, and these most often start in childhood. Therapeutic strategies will need to target children with this disease, perhaps upon evidence of a first bleed. At the same time, the high lesion burden in murine models provides an opportunity to detect and optimize therapeutic benefit in the preclinical setting. And fewer subjects would be needed to demonstrate a treatment effect in clinical trials in view of the high rate of lesion genesis in man, and the frequency of clinically significant hemorrhages (particularly rebleeds). ROCK inhibition therapy is particularly promising, and should be explored along with broader Rho inhibition, documented in pleiotropic effects of statins³⁵. There has been increasing experience with statin use in childhood, making this therapeutic venue quite realistic, if a therapeutic effect and safety of statins are demonstrated in animal models. Brain permeability and other ROCK activity biomarkers³⁶ may help with detecting treatment effect, and with calibrating therapy. The association of brain permeability by MRI with ROCK activity is being investigated in human with familial CCMs. Other therapeutic venues with immune modulation^{37, 38} and other signaling targets^{4, 20, 39, 40} may realistically be screened given the penetrance of disease in murine models recapitulating the human disease. And these may be carefully optimized for clinical trials.

Supplementary Material

Refer to Web version on PubMed Central for supplementary material.

ACKNOWLEDGMENTS

This work was supported in part by the National Institutes of Health [grant numbers NS077957 to I.A.A. and D.A.Ma., 5K01HL092599-04 to R.A.S.], American Heart Association [grant number 12BGIA9850013 to R.A.S.] and by the Bill and Judy Davis Research Fund in Neurovascular Research at the University of Chicago. Recruitment efforts and patient records were provided by CCM3 Action and Angioma Alliance's DNA/Tissue Bank.

REFERENCES

1. Maraire JN, Awad IA. Intracranial cavernous malformations: Lesion behavior and management strategies. *Neurosurgery*. 1995; 37:591–605. [PubMed: 8559286]
2. Bergametti F, Denier C, Labauge P, et al. Mutations within the programmed cell death 10 gene cause cerebral cavernous malformations. *Am J Hum Genet*. 2005; 76:42–51. [PubMed: 15543491]
3. McDonald DA, Shi C, Shenkar R, et al. Fasudil decreases lesion burden in a murine model of cerebral cavernous malformation disease. *Stroke*. 2012; 43:571–574. [PubMed: 22034008]
4. Maddaluno L, Rudini N, Cuttano R, et al. Endmt contributes to the onset and progression of cerebral cavernous malformations. *Nature*. 2013; 498:492–496. [PubMed: 23748444]
5. Li DY, Whitehead KJ. Evaluating strategies for the treatment of cerebral cavernous malformations. *Stroke*. 2010; 41:S92–94. [PubMed: 20876517]
6. Kondziolka D, Monaco EA 3rd, Lunsford LD. Cavernous malformations and hemorrhage risk. *Prog Neurol Surg*. 2013; 27:141–146. [PubMed: 23258518]
7. Al-Shahi Salman R, Hall JM, Horne MA, et al. Untreated clinical course of cerebral cavernous malformations: A prospective, population-based cohort study. *Lancet Neurol*. 2012; 11:217–224. [PubMed: 22297119]
8. Al-Shahi Salman R, Berg MJ, Morrison L, Awad IA. Hemorrhage from cavernous malformations of the brain: Definition and reporting standards. Angioma alliance scientific advisory board. *Stroke*. 2008; 39:3222–3230. [PubMed: 18974380]
9. Gault J, Sain S, Hu LJ, Awad IA. Spectrum of genotype and clinical manifestations in cerebral cavernous malformations. *Neurosurgery*. 2006; 59:1278–1285. [PubMed: 17277691]
10. D'Angelo R, Marini V, Rinaldi C, et al. Mutation analysis of ccm1, ccm2 and ccm3 genes in a cohort of italian patients with cerebral cavernous malformation. *Brain Pathol*. 2011; 21:215–224. [PubMed: 21029238]
11. Denier C, Labauge P, Bergametti F, et al. Genotype-phenotype correlations in cerebral cavernous malformations patients. *Ann Neurol*. 2006; 60:550–556. [PubMed: 17041941]
12. Riant F, Bergametti F, Fournier HD, et al. Ccm3 mutations are associated with early-onset cerebral hemorrhage and multiple meningiomas. *Mol Syndromol*. 2013; 4:165–172. [PubMed: 23801932]
13. Louvi A, Nishimura S, Gunel M. Ccm3, a gene associated with cerebral cavernous malformations, is required for neuronal migration. *Development*. 2014; 141:1404–1415. [PubMed: 24595293]
14. Borikova AL, Dibble CF, Sciaky N, et al. Rho kinase inhibition rescues the endothelial cell cerebral cavernous malformation phenotype. *J Biol Chem*. 2010; 285:11760–11764. [PubMed: 20181950]
15. Stockton RA, Shenkar R, Awad IA, Ginsberg MH. Cerebral cavernous malformations proteins inhibit rho kinase to stabilize vascular integrity. *J Exp Med*. 2010; 207:881–896. [PubMed: 20308363]
16. Chan AC, Drakos SG, Ruiz OE, et al. Mutations in 2 distinct genetic pathways result in cerebral cavernous malformations in mice. *J Clin Invest*. 2011; 121:1871–1881. [PubMed: 21490399]
17. Fidalgo M, Fraile M, Pires A, Force T, Pombo C, Zalvide J. Ccm3/pdcd10 stabilizes gckiii proteins to promote golgi assembly and cell orientation. *J Cell Sci*. 2010; 123:1274–1284. [PubMed: 20332113]
18. You C, Sandalcioglu IE, Dammann P, Felbor U, Sure U, Zhu Y. Loss of ccm3 impairs dll4-notch signalling: Implication in endothelial angiogenesis and in inherited cerebral cavernous malformations. *J Cell Mol Med*. 2013; 17:407–418. [PubMed: 23388056]

19. Yoruk B, Gillers BS, Chi NC, Scott IC. Ccm3 functions in a manner distinct from ccm1 and ccm2 in a zebrafish model of ccm vascular disease. *Dev Biol.* 2012; 362:121–131. [PubMed: 22182521]
20. Hwang J, Pallas DC. Stripak complexes: Structure, biological function, and involvement in human diseases. *Int J Biochem Cell Biol.* 2014; 47:118–148. [PubMed: 24333164]
21. McDonald DA, Shenkar R, Shi C, et al. A novel mouse model of cerebral cavernous malformations based on the two-hit mutation hypothesis recapitulates the human disease. *Hum Mol Genet.* 2011; 20:211–222. [PubMed: 20940147]
22. Ceccarelli DF, Laister RC, Mulligan VK, et al. Ccm3/pdcd10 heterodimerizes with germinal center kinase iii (gckiii) proteins using a mechanism analogous to ccm3 homodimerization. *J Biol Chem.* 2011; 286:25056–25064. [PubMed: 21561863]
23. Gross BA, Lin N, Du R, Day AL. The natural history of intracranial cavernous malformations. *Neurosurg Focus.* 2011; 30:E24. [PubMed: 21631226]
24. Labauge P, Brunereau L, Laberge S, Houtteville JP. Prospective follow-up of 33 asymptomatic patients with familial cerebral cavernous malformations. *Neurology.* 2001; 57:1825–1828. [PubMed: 11723271]
25. Zabramski JM, Wascher TM, Spetzler RF, et al. The natural history of familial cavernous malformations: Results of an ongoing study. *J Neurosurg.* 1994; 80:422–432. [PubMed: 8113854]
26. Whitehead KJ, Chan AC, Navankasattusas S, et al. The cerebral cavernous malformation signaling pathway promotes vascular integrity via rho gtpases. *Nat Med.* 2009; 15:177–184. [PubMed: 19151728]
27. Grassie ME, Moffat LD, Walsh MP, MacDonald JA. The myosin phosphatase targeting protein (mypt) family: A regulated mechanism for achieving substrate specificity of the catalytic subunit of protein phosphatase type 1delta. *Arch Biochem Biophys.* 2011; 510:147–159. [PubMed: 21291858]
28. Muranyi A, Derkach D, Erdodi F, Kiss A, Ito M, Hartshorne DJ. Phosphorylation of thr695 and thr850 on the myosin phosphatase target subunit: Inhibitory effects and occurrence in a7r5 cells. *FEBS Lett.* 2005; 579:6611–6615. [PubMed: 16297917]
29. Shenkar R, Venkatasubramanian PN, Wyrwicz AM, et al. Advanced magnetic resonance imaging of cerebral cavernous malformations: Part ii. Imaging of lesions in murine models. *Neurosurgery.* 2008; 63:790–798. [PubMed: 18981891]
30. Gault J, Shenkar R, Recksiek P, Awad IA. Biallelic somatic and germ line ccm1 truncating mutations in a cerebral cavernous malformation lesion. *Stroke.* 2005; 36:872–874. [PubMed: 15718512]
31. Akers AL, Johnson E, Steinberg GK, Zabramski JM, Marchuk DA. Biallelic somatic and germline mutations in cerebral cavernous malformations (ccms): Evidence for a two-hit mechanism of ccm pathogenesis. *Hum Mol Genet.* 2009; 18:919–930. [PubMed: 19088123]
32. Liquori CL, Berg MJ, Squitieri F, et al. Low frequency of pdcd10 mutations in a panel of ccm3 probands: Potential for a fourth ccm locus. *Hum Mutat.* 2006; 27:118. [PubMed: 16329096]
33. Sirvente J, Enjolras O, Wassef M, Tournier-Lasserre E, Labauge P. Frequency and phenotypes of cutaneous vascular malformations in a consecutive series of 417 patients with familial cerebral cavernous malformations. *J Eur Acad Dermatol Venereol.* 2009; 23:1066–1072. [PubMed: 19453802]
34. Huynh J, Nishimura N, Rana K, et al. Age-related intimal stiffening enhances endothelial permeability and leukocyte transmigration. *Sci Transl Med.* 2011; 3:112ra122.
35. Zhou Q, Liao JK. Pleiotropic effects of statins. -basic research and clinical perspectives- *Circ J.* 2010; 74:818–826. [PubMed: 20424337]
36. Liu PY, Liao JK. A method for measuring rho kinase activity in tissues and cells. *Methods Enzymol.* 2008; 439:181–189. [PubMed: 18374165]
37. Zhang Y, Tang W, Zhang H, et al. A network of interactions enables ccm3 and stk24 to coordinate unc13d-driven vesicle exocytosis in neutrophils. *Dev Cell.* 2013; 27:215–226. [PubMed: 24176643]
38. Shi C, Shenkar R, Du H, et al. Immune response in human cerebral cavernous malformations. *Stroke.* 2009; 40:1659–1665. [PubMed: 19286587]

39. Fisher OS, Boggon TJ. Signaling pathways and the cerebral cavernous malformations proteins: Lessons from structural biology. *Cell Mol Life Sci.* 2013
40. Bacigaluppi S, Retta SF, Pileggi S, et al. Genetic and cellular basis of cerebral cavernous malformations: Implications for clinical management. *Clin Genet.* 2013; 83:7–14. [PubMed: 22510019]

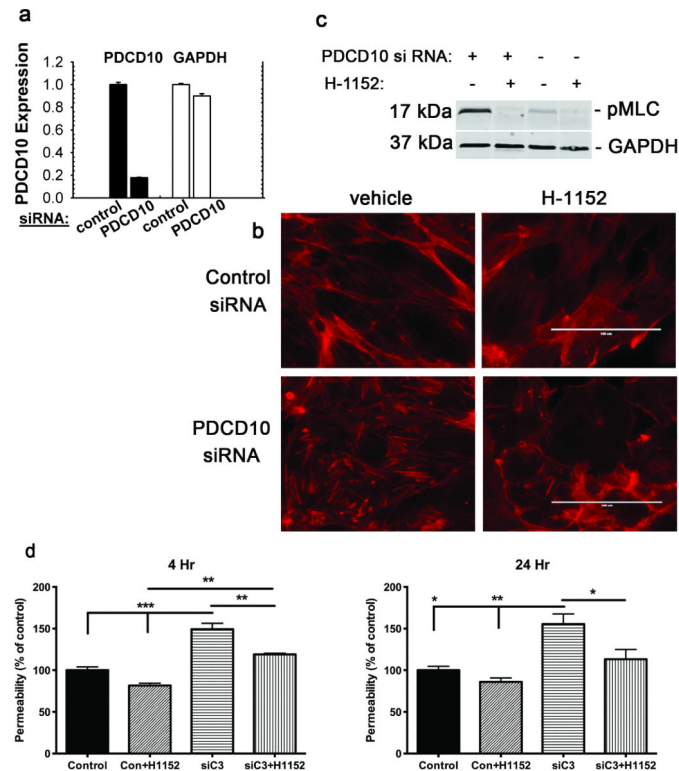


Figure 1. PDCD10 suppresses stress fibers, ROCK activity and permeability *in vitro*

HUVECs were treated with control or *PDCD10* siRNA. (A) *PDCD10* gene expression is reduced by 80% by *PDCD10* siRNA in HUVECs as compared to those treated with control siRNA. Data bars are means \pm SE. (B) Increased f-actin stress fibers by *PDCD10* depletion is blunted by the ROCK inhibitor H-1152. Bar, 100 μ m. (C) Increased pMLC activity by *PDCD10* depletion is reversed by H-1152. (D) *PDCD10* depletion during 4 and 24 hours increases monolayer permeability in transwell assays. H-1152 treatment reverses this increase, implying that *PDCD10* inhibits ROCK-mediated monolayer leak. Data bars are means \pm SE of $n = 3$. Analysis by ANOVA indicates * $P < 0.05$, ** $P < 0.01$, *** $P < 0.001$.

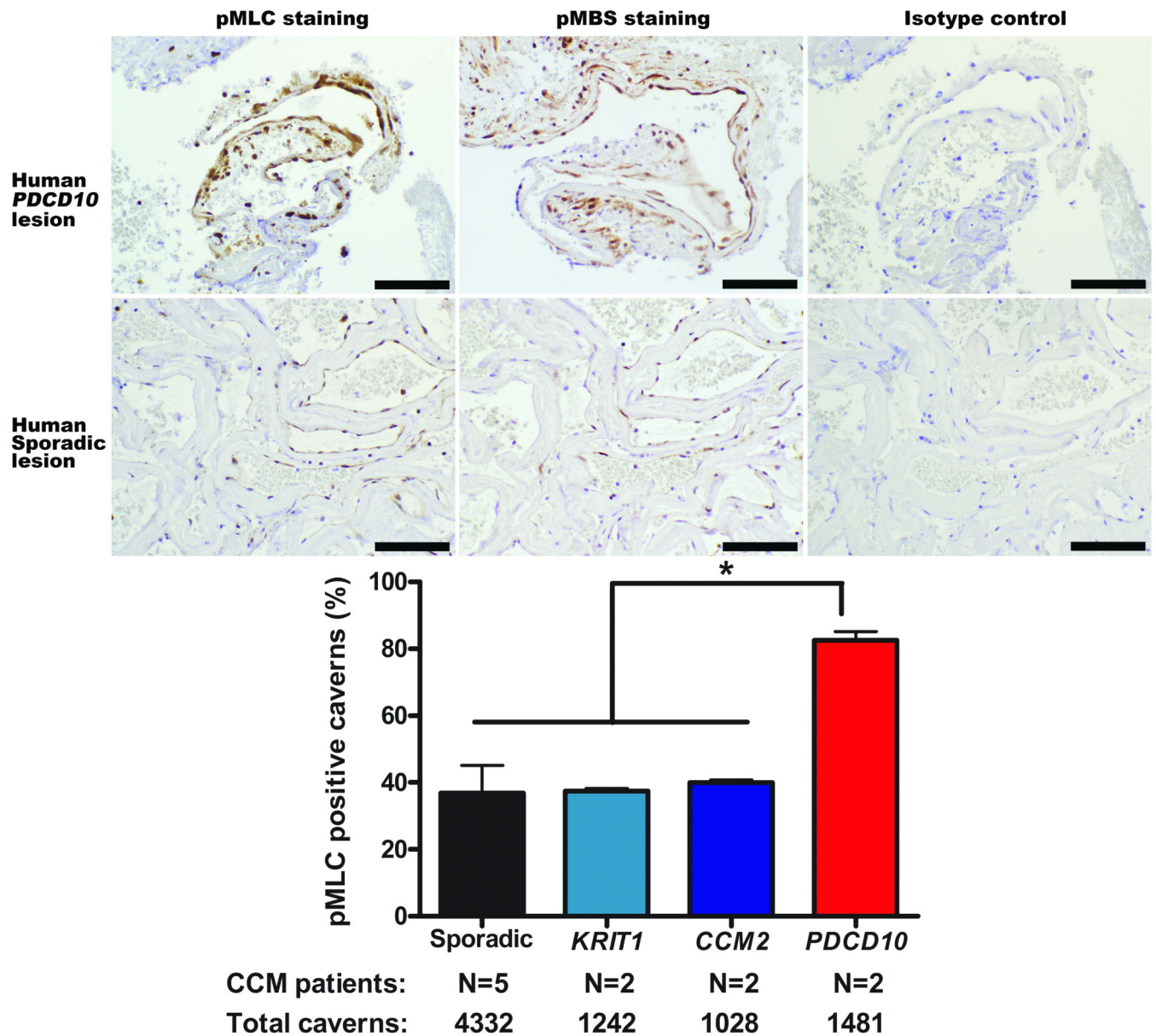


Figure 2. ROCK activity in CCM lesions from human subjects

There is greater ROCK activity in human *PDCD10* CCM lesions than in human sporadic lesions as shown by brown pMLC and pMBS staining. Bars are 100 μ m. The histogram shows that twice as many caverns have at least one endothelial cell stained with pMLC in human *PDCD10* CCM lesions than in human *KRIT1*, *CCM2* and sporadic lesions (* $P < 0.05$). Data bars are means \pm SE.

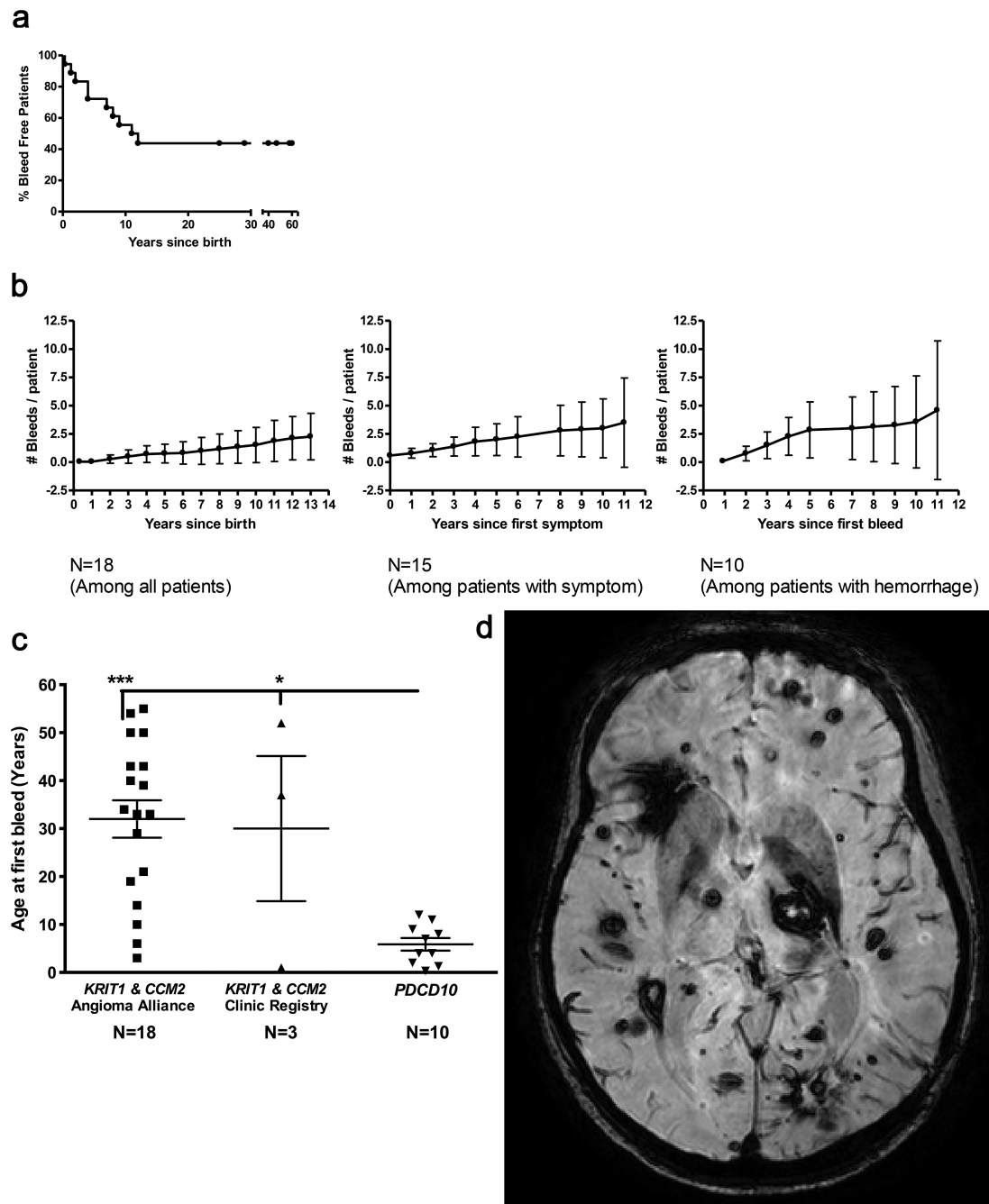


Figure 3. *PDCD10* patients show a more aggressive phenotype

(A) Percent of bleed free *PDCD10* patients versus age, showing high bleeding propensity in the first decade of life, leveling off in the teen years. The time of hemorrhage has been established for every adjudicated bleed. (B) Number of bleeds per *PDCD10* patient (mean plotted, with standard error bar) vs. years since birth, after first symptom onset, and after first hemorrhage. (C) The age at first bleed is lower in *PDCD10* patients than in *KRIT1* and *CCM2* patients. Data bars are means \pm SE. (D) An SWI scan showing high lesion burden in a *PDCD10* patient.

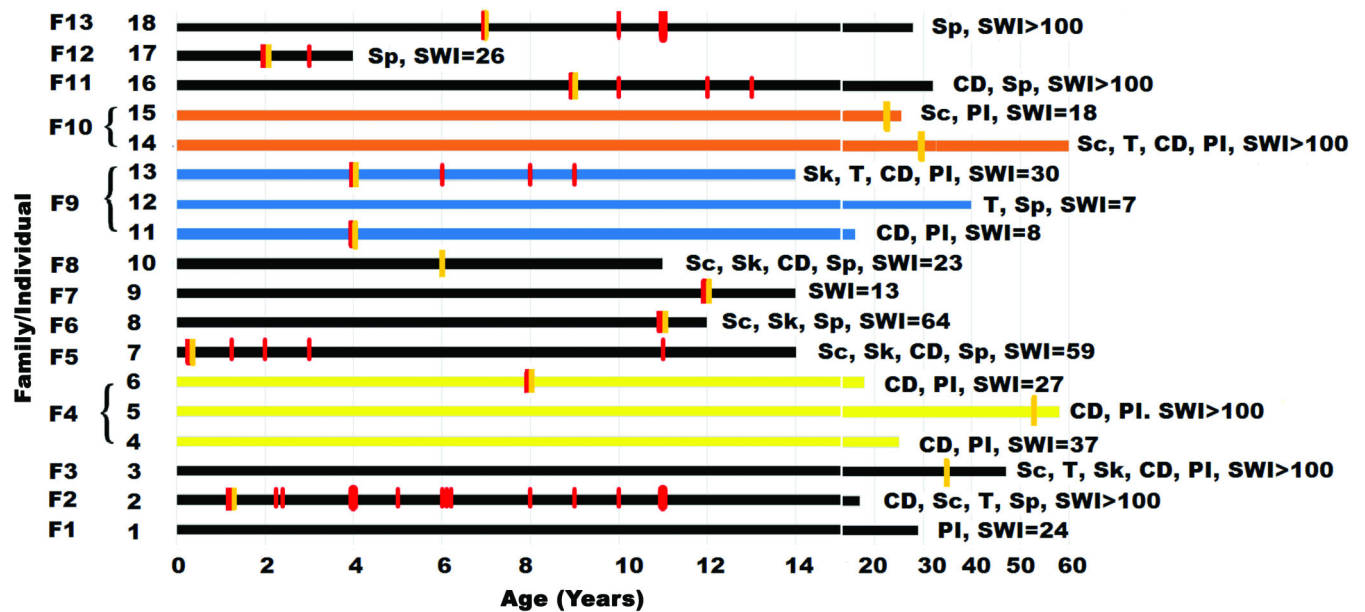


Figure 4. Phenotypic profile of *PDCD10* patients

The cases are grouped by their respective proband (F1 to F12). Each subject's lesion burden and clinical associations is indicated. Each symptomatic bleed is noted by a red vertical bar during the lifespan of each subject. First symptomatic onset is noted by a yellow vertical bar. Sp = spontaneous mutation, PI = parental inheritance, CD = cognitive decline, Sk = skin manifestation, Sc = scoliosis, T = tumor, SWI = number of lesions on susceptibility weighted imaging.

Table 1

PDCD10 proband mutations all lead to loss of function alleles.

Family	Mutation	Effect
1	c.180delA, p.60fsX64	nonsense
2	c.474+5G>A	splicing
3	c.474+1G>A	splicing
4	c.322C>T; p.Arg108Stop	nonsense
5	c.608T>G; p.Leu203Stop	nonsense
6	c.474+5G>A	splicing
7	c.474+5 G>A	splicing
8	c.124C>T; p.Gln42Stop	nonsense
9	c.474+1G>A	splicing
10	c.131T>C; p.Leu44Pro	missense
11	c.501delT, p.167fsX168	nonsense
12	c.103C>T; p.Arg35Stop	nonsense
13	c.475-2A>G	splicing